

Validation of MODIS aerosol optical depth retrieval over land

D. A. Chu^{1,2}, Y. J. Kaufman¹, C. Ichoku^{1,2}, L. A. Remer¹, D. Tanre³, B. N. Holben⁴

Abstract. Aerosol optical depths (τ_a) are derived operationally for the first time from the MODIS (Moderate Resolution Imaging Spectroradiometer) measurements over vegetated and partially vegetated land at 0.47 and 0.66 μm wavelengths. The extensive validation made during July - September 2000 encompasses 315 co-located τ_a in space and time derived by MODIS and AERONET (Aerosol Robotic Network) from more than 30 AERONET sites in Europe, Africa, North and South America. The lack of AERONET measurements in East Asia, India and Australia makes this validation unavailable for air pollution and biomass burning aerosols in those regions. In summary, the MODIS aerosol retrievals, except in coastal zones, are found within the retrieval errors of $\Delta\tau_a = \pm 0.05 \pm 0.20\tau_a$. The root mean square (RMS) errors are ≤ 0.1 in the continental inland regions and up to 0.3 in the coastal regions attributed mainly to water contaminated signals. With this validation we believe that the MODIS aerosol products can be used quantitatively for air pollution, fire, and climate studies but with caution for possible presence of residual clouds, snow/ice, and water contamination.

Introduction

The application of satellite data to derive global aerosol properties has advanced dramatically in the last few years. One of the main advancements is the systematic derivation of aerosol over land from MODIS onboard the EOS-Terra satellite launched on December 18, 1999. Since February 24, 2000, MODIS has continuously acquired daily global measurements with thirty-six spectral bands (0.41 - 14 μm) at three different spatial resolutions (250m, 500m and 1 km) [Salomonson *et al.*, 1989]. We retrieve aerosol properties over both land [Kaufman *et al.*, 1997a] and ocean [Tanre *et al.*, 1997] using seven well calibrated spectral channels in the solar spectrum region (0.47 - 2.1 μm). In this paper we present the first comprehensive validation of the MODIS-derived τ_a over land.

The MODIS retrieval of τ_a over land employs primarily three spectral channels centered at 0.47, 0.66, and 2.1 μm at 500m resolution. A short description of the MODIS aerosol algorithm presented here follows Kaufman *et al.* [1997a]. In a 10 km \times 10 km grid box, cloud-free pixels are first selected using the multi-spectral MODIS cloud mask [Ackerman *et al.*, 1998]. The cloud mask uses more than twenty tests including cirrus detection test to indicate a cloudy or clear pixel at 1 \times 1 km resolution. Fine-mode aerosols are transparent at 2.1 μm wavelength. Therefore it allows the direct observation of land surface. The empirical relationships developed over vegetated surface are used to estimate the surface reflectance (ρ_s) at 0.47 μm and at 0.66 μm from the measurements at 2.1 μm ($\rho_s^{0.47\mu\text{m}}/\rho_s^{2.1\mu\text{m}} = 0.25$ and $\rho_s^{0.66\mu\text{m}}/\rho_s^{2.1\mu\text{m}} = 0.5$) [Kaufman *et al.*, 1997b]. To minimize the error, the MODIS aerosol retrievals over land are limited to pixels of $\rho_s^{2.1\mu\text{m}} < 0.15$. Snow/ice and water covered surfaces are excluded because the empirical relationships given above are invalid over those regions. The selected cloud-free dark pixels in the grid box may still be partially contaminated by sub-pixel clouds, snow/ice, or soil types that do not fit the empirical relationship (e.g. red soil [Gazbe *et al.*, 2001]). Thus only the 10-40 percentile of

MODIS measured radiance is used. The overall retrieval errors were estimated to be $\Delta\tau_a = \pm 0.05 \pm 0.20\tau_a$ ($\sim 100\%$ error for $\tau_a = 0.05$). Larger error of ± 0.3 is found for dust particle when using the 2.1 μm channel [Kaufman *et al.*, 2001] as opposed to ± 0.05 for urban/industrial and biomass burning aerosols. To distinguish between dust and non-dust aerosols, the ratio of aerosol path radiance at 0.66 and 0.47 μm is used. Sulfate and smoke aerosols that can not be distinguished by the path radiance ratio are separated a priori according to the geographic locations and seasons of their emission sources. The details of the determination of aerosol types (including the mixture of different aerosols) and the aerosol models used by the retrieval algorithm can be found in Kaufman *et al.* [1997a].

The β release of MODIS level-2 (10 km \times 10 km) granule-based (granule: a 5-minute segment of one MODIS orbital data) and level-3 (1 $^\circ$ \times 1 $^\circ$) gridded aerosol products was to provide a preview before quality assurance. The validation data presented here are the basis for the release of the first version of validated products.

Validation approach

In order to take into account both spatial and temporal variabilities of aerosol distribution, the MODIS retrievals at 10 km \times 10 km resolution and the AERONET direct Sun measurements at 15-minute intervals [Holben *et al.*, 1998] need to be co-located in space and time. We require at least 2 out of possible 5 AERONET measurements within ± 30 min of MODIS overpasses and at least 5 out of possible 25 MODIS retrievals in a square box of 50 km \times 50 km centered over AERONET sites. The mean values of the co-located spatial and temporal ensemble are then used in linear regression analysis and in calculating RMS errors. The AERONET level 1.5 data are cloud screened. Though the level 2.0 data provide final calibration, they are not available in real time. Therefore the level 1.5 data (instead of level 2.0) are used in the operational MODIS aerosol validation scheme.

Validation of Aerosol Optical Depth

Figure 1 displays the frequency map of MODIS aerosol retrievals over land as derived using the level-3 daily aerosol products from July to September 2000. Superimposed on Figure 1 are the locations of the AERONET sites included in this validation. The MODIS aerosol retrievals cover approximately 70% of the land surface. The frequency lower than 100% of a given 1 $^\circ$ \times 1 $^\circ$ grid box is due to clouds cover, non-vegetated surfaces, or missing data. Most of the regions with dust occurrence are excluded due to high brightness of desert surface (e.g., Sahara Desert). Also excluded are snow/ice-covered regions (e.g., Antarctica and Greenland) - too bright in the visible wavelength to derive aerosol optical depth. At high latitudes, more retrievals are seen because of the overlapped satellite orbits.

A total of 315 points representing more than 30 AERONET sites meet our match-up criteria for the MODIS- and AERONET-derived τ_a in the period of July - September, 2000. Small islands, such as Barbados, Bermuda, Cape Verde, Hawaii, etc. are

too small for land validation. The slopes (S_i) of linear regression represent systematic biases if differing from 1 and the intercepts (I_c) represent the errors in the ρ_s estimates. Large errors in ρ_s lead to large I_c . The scatter plots in Figures 2(a) and (b) depict overall a very good agreement between MODIS and AERONET with $S_i \sim 0.86$, $I_c \sim 0.02-0.06$, and high correlation coefficients (R) $\sim 0.85-0.91$. Nearly all the points fall within the retrieval errors of $\Delta\tau_a = \pm 0.05 \pm 0.20\tau_a$ and the RMS errors are in the range of 0.07-0.11. Venice and El Arenosillo coastal sites excluded in Figure 2 with larger RMS errors ($\sim 0.2-0.3$) and I_c (~ 0.2) will be discussed later. The systematic biases in MODIS retrievals are mainly due to aerosol model assumptions (deviation of 0-20%), instrument calibration (2-5%), or the choice of the lowest 10-40 percentile of the measurements (0-10%). In the following sub-sections, we examine two regions in detail (1) the continental inland regions of US and west Europe, Brazil and southern Africa, for similar occurrence of the industrial/urban pollution and biomass burning aerosols, and (2) the continental coasts of eastern US and west Europe for the effect of water contamination.

Continental Inland

Figures 3(a) and (b) show the comparison between the MODIS- and AERONET-derived τ_a in east US and in Brazil where pre-launch field experiments took place, with dominant urban/industrial and biomass burning aerosols, respectively. The small values of $I_c \sim 0.01$ in Figures 3(a) and (b) reveal that the vegetated surfaces, such as evergreen, deciduous, mixed forests, and cropland, give the best estimates of ρ_s as anticipated. In terms of S_i , smaller deviations from unity are found at 0.47 μm (≤ 0.05) than at 0.66 μm (> 0.1). The S_i of 0.86 in Figure 3(b) is unexpected because it disagrees with previous validation. In that the single scattering albedo (ω_0) of 0.90 was shown to result in the best fit of τ_a ($S_i \sim 0.97$, $I_c \sim 0.03$, $R \sim 0.98$) derived from MODIS Airborne Simulator and AERONET measurements [Chu *et al.*, 1998]. We assumed the same ω_0 ($= 0.90$) at 0.47 and 0.66 μm despite the recent work of Dubovik *et al.* [2000] that ω_0 may be slightly higher at 0.47 μm than at 0.66 μm . The difference, however, is not significant. Interannual variation in aerosol properties, or stronger calibration drift of AERONET Sun photometers at 0.66 μm [Smirnov *et al.*, private communication] are suspected to be the primary reasons for producing the poorer fit.

The MODIS retrievals in regions with urban/industrial pollution or smoke from biomass burning are based on the aerosol models derived from field measurements in east US and in Brazil. The similar S_i and I_c shown in Figures 3(a) and (c) imply that the differences, if any, in aerosol particle size and chemical composition are too small to affect the retrievals. For biomass burning aerosol, the values of S_i deviating from 1 (0.1 at 0.47 μm and 0.08 at 0.66 μm) in Figure 3(d) are most likely caused by the higher soot concentration from the biomass burning in southern Africa than in South America. In other words, lowering ω_0 will result in a better fit, which is in agreement with the ω_0 values (smaller ω_0 in southern Africa than in South America) derived by Dubovik *et al.* [2000].

Continental Coasts

Surface inhomogeneity or sub-pixel water contamination has a larger effect than we anticipated in continental coastal regions. We examined five AERONET sites: NASA GSFC (US), Maryland Science Center (US), Wallops (US), Venice (Italy),

and El Arenosillo (Spain). Clearly, the values of $I_c \sim 0.18$ and 0.2 derived at Venice and El Arenosillo are twice larger than those of 0.05 and 0.09 at the US coastal sites (see Figures 4(a) and (b)). One can see that the RMS errors are closely associated with the intercepts. The smaller values I_c (< 0.1) resulting from the East Coast of US in July-September (usually dry) are in contrast to earlier results ($\sim 0.15-0.2$) in spring (usually wet) caused by the standing water from frequent rain events.

Spectral Dependence of Aerosol Optical Depth

Ångström exponent (α) is commonly used to describe the spectral dependence of τ_a . For MODIS, α is calculated as follows

$$\alpha = \ln(\tau_a^{0.47\mu\text{m}} / \tau_a^{0.66\mu\text{m}}) / \ln(0.66 / 0.47)$$

where $\tau_a^{0.47\mu\text{m}}$ and $\tau_a^{0.66\mu\text{m}}$ are the MODIS-derived τ_a at 0.47 μm and 0.66 μm , respectively. The uncertainty in surface reflectance is shown to be one of the important factors in the derivation of α . A reasonable fit is found between MODIS- and AERONET- α when $\tau_a^{0.66\mu\text{m}} > 0.2$ ($S_i \sim 0.80$, $I_c \sim 0.14$, $R \sim 0.50$) because of the diminishing effect of the error in surface reflectance estimates (see Figure 5). Other factors affecting the accuracy of α include the uncertainties of aerosol properties, e.g., ω_0 and particle size.

Aerosol Global Distribution

The global monthly means of τ_a and α over land are shown in Figures 6 (a) and (b) for September 2000, respectively. We select the month of September because there are more complete data in September than in July or August. The dry-season biomass burning in Africa and in South America are most visible with means $\sim 0.5-0.7$ compared to the air pollution in Europe and North America with means $\sim 0.2-0.3$ and in China and India with means $\sim 0.4-0.5$. The corresponding α reveals reasonable correlation with the urban/industrial aerosol in North America, Europe, China, and India, and with the biomass-burning aerosol in Brazil and southern Africa. Slightly small α at the boundary of Sahara Desert shows possible mixture of urban/industrial or biomass burning aerosols with dust particles.

Concluding Remarks

The MODIS aerosol retrievals over land meet our expectation with unprecedented accuracy. With the continuous refinements in instrument calibration, we expect the quality of the aerosol products to improve with time. However, several sources of the errors in aerosol retrieval remain to be solved, such as the sub-pixel cloud, snow/ice, and water contamination, the uncertainties in heterogeneous surface reflectance, and the aerosol properties beyond the scope of the assumptions of aerosol models. The scenarios of dust outbreaks and air pollution in East Asia are good test beds for testing the surface reflectance estimation and aerosol models. The ACE-Asia field campaign, which took place in March - May 2001, shall provide the important insight for evaluating the MODIS aerosol retrievals in that region.

Acknowledgements The authors would like to thank the Goddard DAAC and MODIS software development and support team for processing MODIS level-1, level-2, and level-3 data, and the AERONET PIs for collecting the aerosol observations around the world.

References

- Ackerman, S. A. et al., Discriminating clear-sky from clouds with MODIS, *J. Geophys. Res.*, 103, 32,141-32,158, 1998.
- Chu, D. A. et al., Remote sensing of smoke from MODIS airborne simulator during SCAR-B experiment, *J. Geophys. Res.*, 103, 31,979-31,987, 1998.
- Dubovik, O. et al., Accuracy assessments of aerosol properties retrieved from AERONET Sun and sky-radiance measurements, *J. Geophys. Res.*, in press, 2000.
- Gatebe, C. K. et al., Sensitivity of off-nadir zenith angle to correlation between visible and near-infrared reflectance for use in remote sensing of aerosol over land, *IEEE Trans. on Geos. and Remote Sens.*, 39, 4, 805-819, 2001.
- Holben, B. N. et al., AERONET-A federated instrument network and data archive for aerosol characterization, *Rem. Sens. Environ.*, 66, 1-16, 1998.
- Kaufman, Y. J. et al., Operational remote sensing of tropospheric aerosol over the land from EOS-MODIS, *J. Geophys. Res.*, 102, 17,051-17,061, 1997a.
- Kaufman, Y. J. et al., The MODIS 2.1 μm channel—Correlation with visible reflectance for use in remote sensing of aerosol, *IEEE Trans. Geosci. Remote Sens.*, 35, 5, 1286-1298, 1997b.
- Kaufman, Y. J. et al., Absorption of sunlight by dust as inferred from satellite and ground-based remote sensing, *Geophys. Res. Lett.*, 28, 8, 1479-1482, 2001.
- Salomonson, V. et al., MODIS Advanced facility instrument for studies of the earth as a system. *IEEE Transactions on Geoscience and Remote Sensing*, 27(2), 145-153, 1989.
- Tanré, D. et al, Remote sensing of aerosol over oceans from EOS-MODIS, *JGR-Atmospheres*, special issue on remote sensing of aerosol and atmospheric corrections, 102, 16971-16988, 1997.

Figure Captions

Figure 1. Frequency map of MODIS aerosol retrievals over land derived from MODIS $1^\circ \times 1^\circ$ level-3 daily products between July and September 2000. The white circles depict the locations of the AERONET Sun photometer sites.

Figure 2. Global comparison of MODIS- and AERONET-derived τ_a at 0.47 and 0.66 μm wavelengths, encompassing 315 points from more than 30 AERONET sites but excluding Venice and El Arenosillo coastal sites. The solid lines represents the slopes of linear regression and the dot lines the retrieval errors of $\Delta\tau_a = \pm 0.05 \pm 0.20\tau_a$. Standard deviations are shown as the error bars in x (AERONET) and y (MODIS) directions.

Figure 3. Regional comparison of MODIS- and AERONET-derived τ_a at 0.47 and 0.66 μm wavelengths in continental inland regions: (a) eastern US, (b) Brazil, (c) west Europe, and (d) southern Africa. The solid lines represents the slopes of linear regression and the dot lines the retrieval errors of $\Delta\tau_a = \pm 0.05 \pm 0.20\tau_a$. Standard deviations are shown as the error

bars in x (AERONET) and y (MODIS) directions.

Figure 4. Regional comparison MODIS- and AERONET-derived τ_a at 0.47 and 0.66 μm wavelengths in the continental coastal zones: (a) Venice and El Arenosillo and (b) NASA GSFC, Wallops, and Maryland Science Center. The solid lines represents the slopes of linear regression and the dot lines the retrieval errors of $\Delta\tau_a = \pm 0.05 \pm 0.20\tau_a$. Standard deviations are shown as the error bars in x (AERONET) and y (MODIS) directions.

Figure 5. Comparison of MODIS and AERONET-derived α when $\tau_a^{0.66\mu\text{m}} > 0.2$ (red: biomass-burning aerosol; blue: industrial/urban aerosol; green: mixed aerosol with dust particle; white: biomass-burning or industrial/urban aerosols outside the regions as shown in Figure 3).

Figure 6. Global monthly mean of (a) τ_a (at 0.55 μm) and (b) α derived from MODIS $1^\circ \times 1^\circ$ level-3 daily products of September 2000.

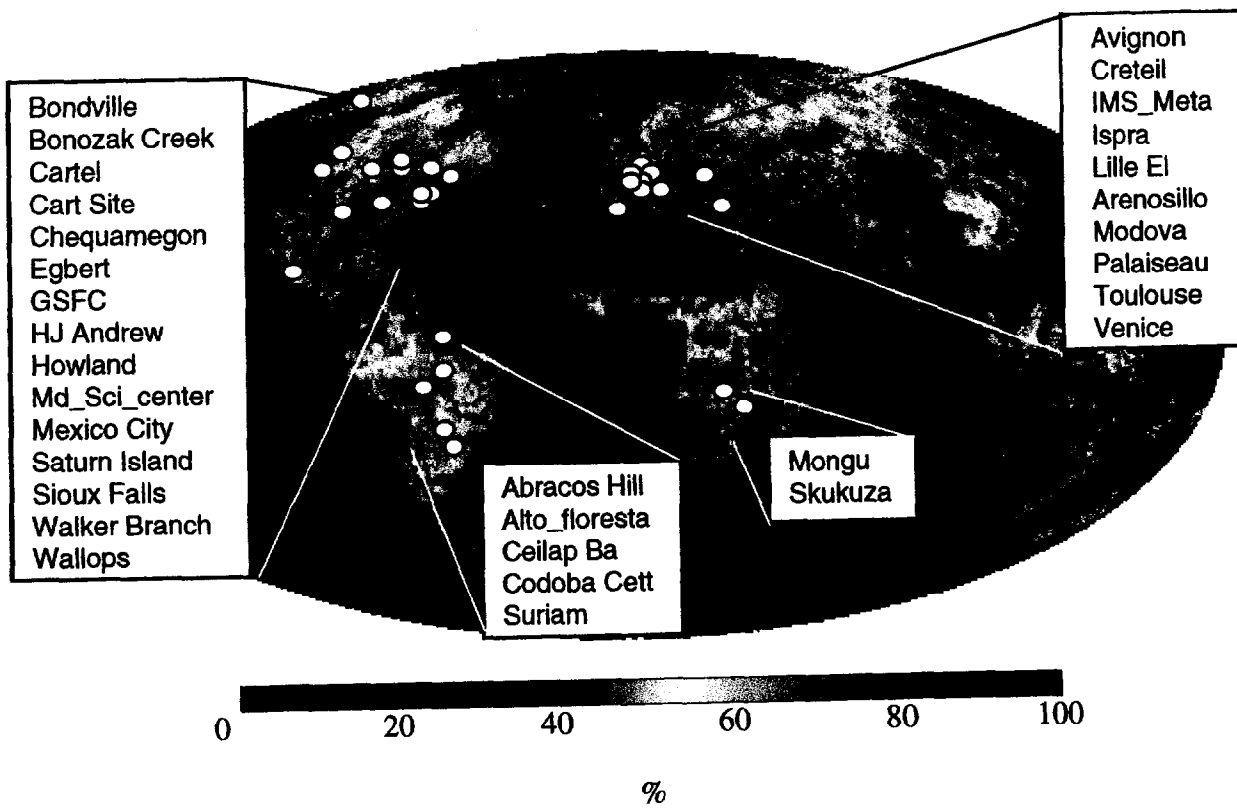
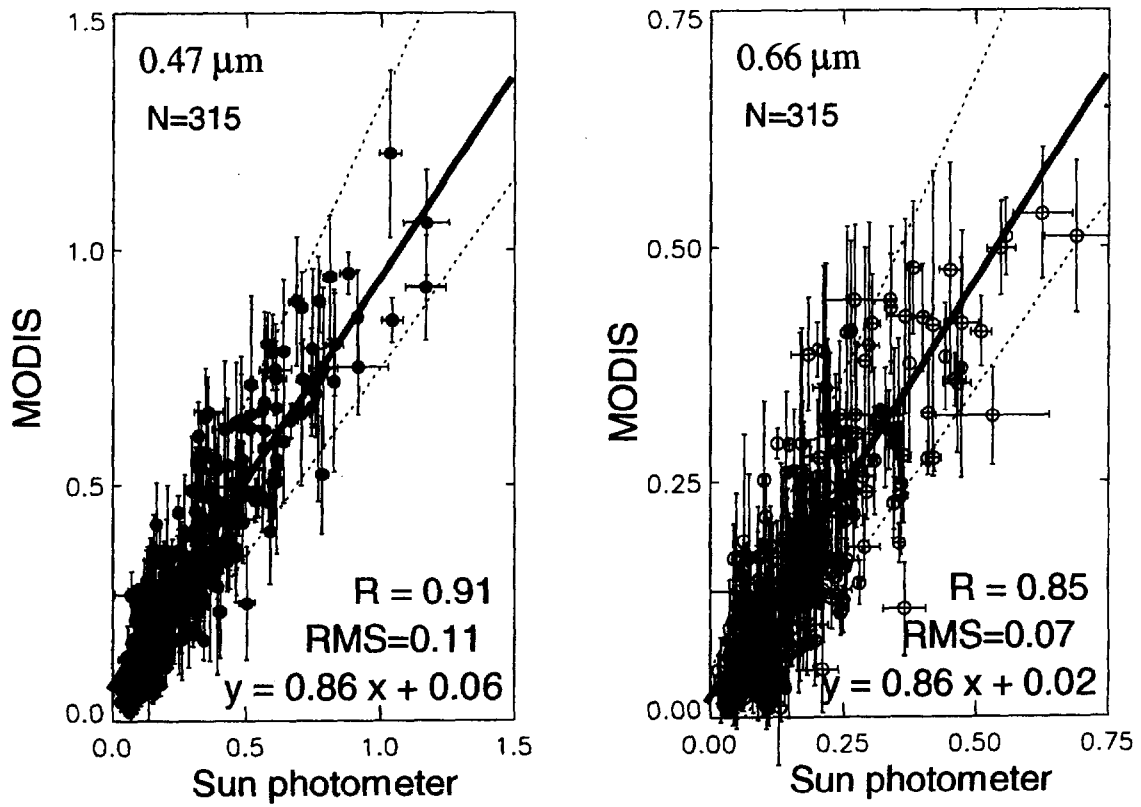


Figure 1



Excluding Venice and El Arenosillo sites

Figure 2

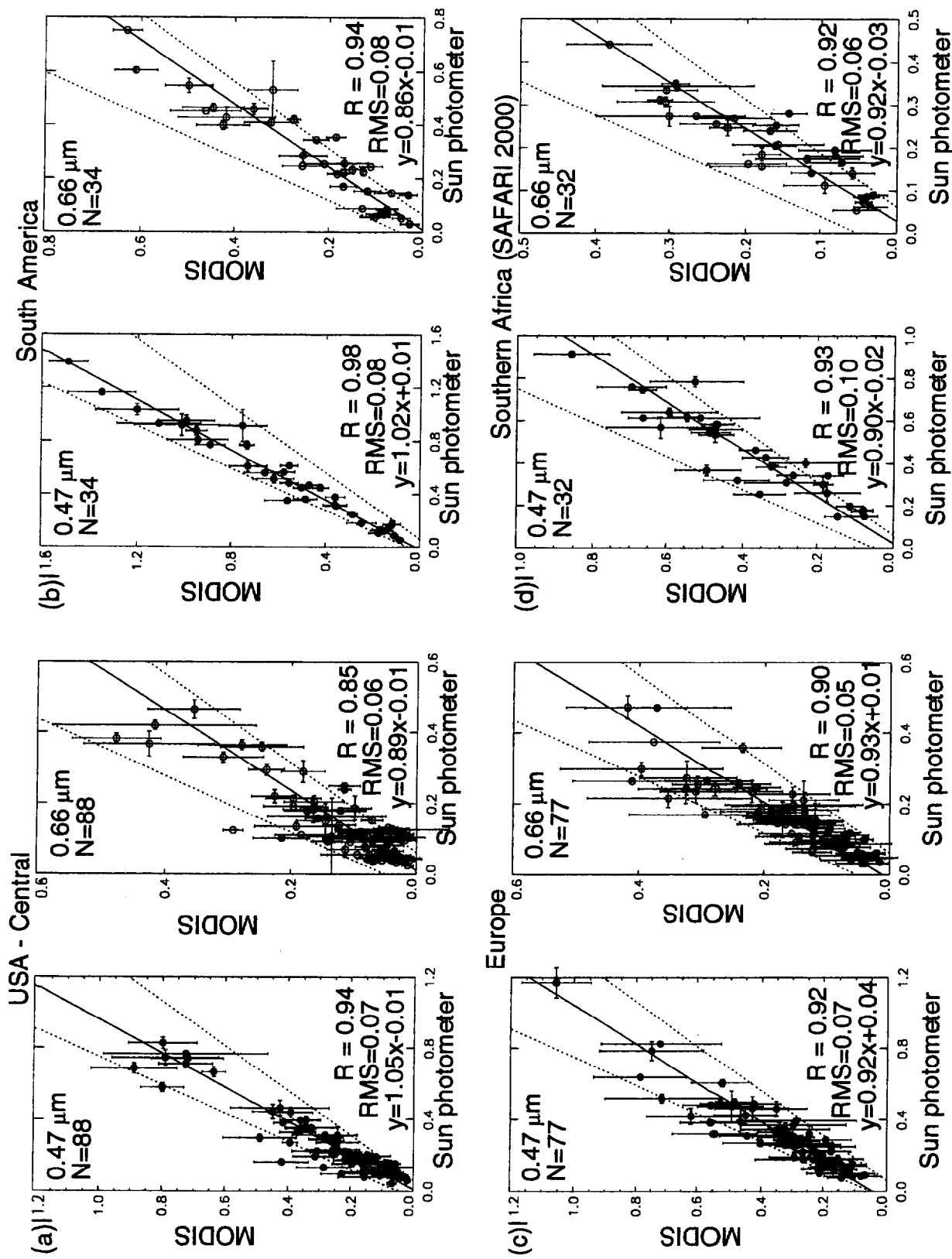


Figure 3

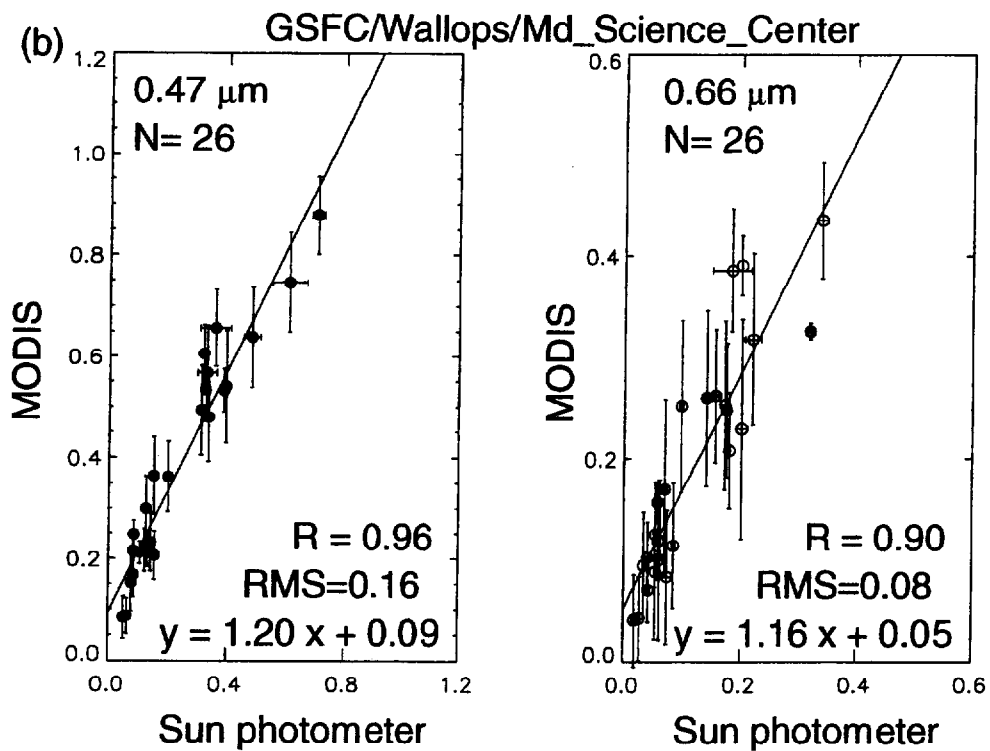
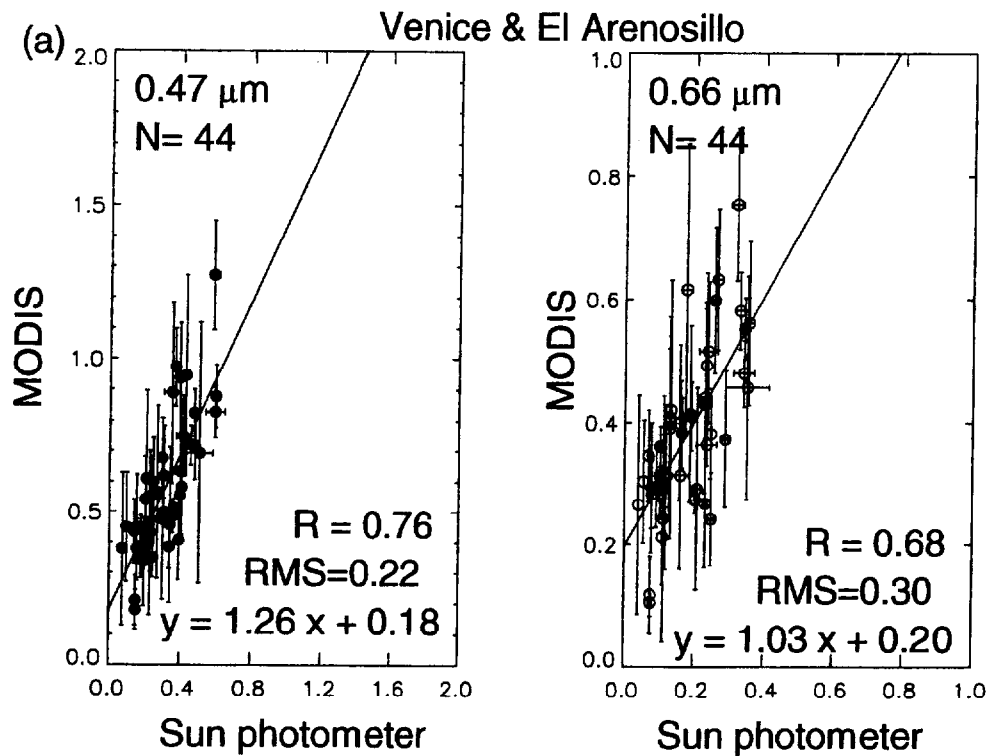


Figure 4(a) & (b)

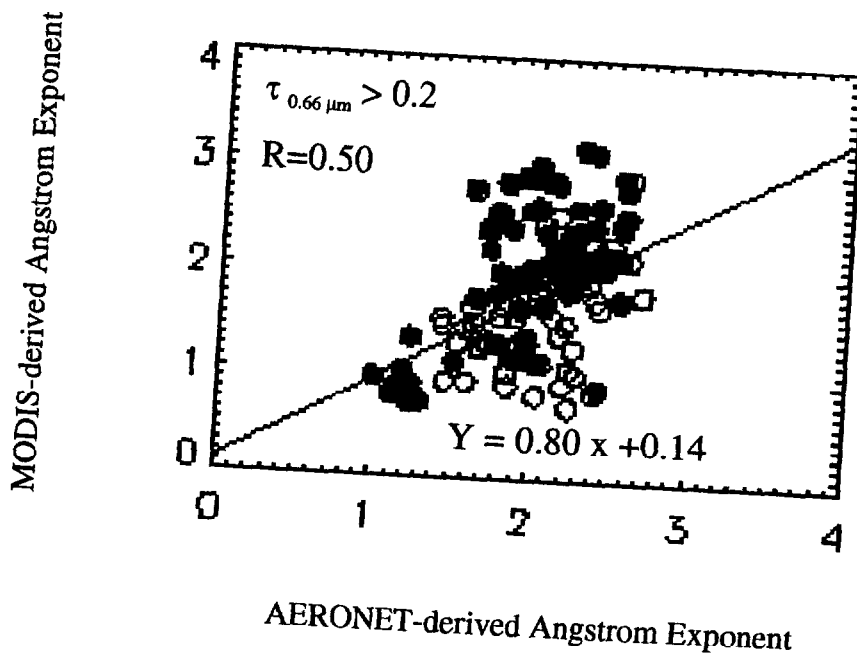
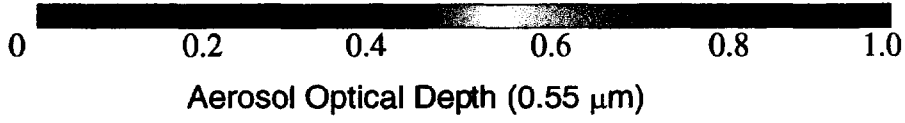


Figure 5

(a)



(b)

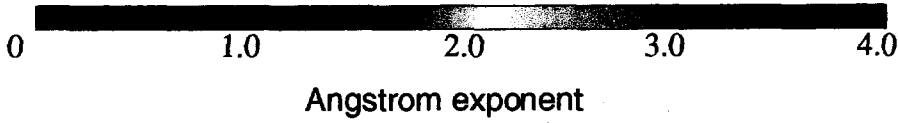
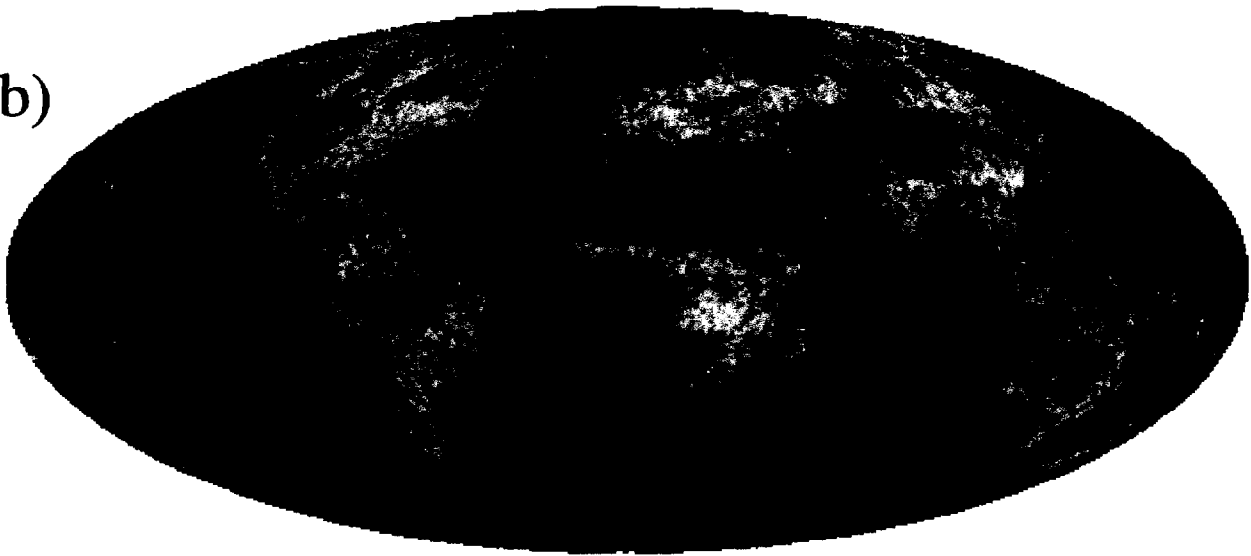


Figure 6(a) & (b)